

Article ID: 1003-7837(2005)02,03-0093-09

Study on spinel-based inert anode for aluminium electrolysis

WANG Zhao-wen(王兆文), HU Xian-wei(胡宪伟), LUO Tao(罗涛),
GAO Bing-liang(高炳亮), SHI Zhong-ning(石忠宁), QIU Zhu-xian(邱竹贤)

(School of Materials & Metallurgy of Northeastern University, Shenyang 110004, China)

Abstract: Hot press-sintering was adopted to fabricate inert cermets anodes based on the nickel aluminate and nickel ferrite for use in aluminum electrolysis research. The density of samples, fabricated by hot pressing, is close to the theoretic density. At 900°C, the electrical conductivity of the nickel aluminate spinel-based inert anode is more than $80 \text{ S} \cdot \text{cm}^{-1}$ and that of nickel ferrite ranged from $40 \text{ S} \cdot \text{cm}^{-1}$ to $80 \text{ S} \cdot \text{cm}^{-1}$. Reasons for anode corrosion were analyzed after electrolysis experiments. Effect of anode current on nickel ferrite-based and the reason for it were studied. A theory is that a more uniform metal distribution by improving the hot pressing process gives increased corrosion resistance of the anode.

Key words: nickel aluminate; nickel ferrite; aluminium electrolysis; electrical conductivity; corrosion resistance

CLC number: TF111.52 **Document code:** A

1 Introduction

Since the Hall-Heroult process was applied in aluminium production, an inert anode was always the target that the aluminium industry is seeking for in the new technology field. The greenhouse gases CO_2 and the fluoride CF_x emitted from the present carbon anodes, give a huge pressure on the environment. The application of inert anodes will help us go through this trouble: a cell with inert anodes emits oxygen instead of CO_2 and other nocuous gases; the new type of cell with inert anodes and other new technologies would save energy^[1-8].

There are three types of inert anode materials: alloy materials, oxide ceramic materials and cermet materials^[9-13]. The choice of cermet materials is apt to the compound materials of spinel and metals, and then the inert anode reaches the optimum point of corrosion resistance performance of the ceramic and the electrical conduction performance of the metal. At present nickel ferrite (NiFe_2O_4) is widely studied as matrix by researches. It has the advantage of a low solubility of Fe_2O_3 and NiO in the molten salt electrolyte^[5], and then the corrosion resistance of the spinel ceramic can be enhanced. Nickel aluminate (NiAl_2O_4) is another important kind of material as inert anode matrix. Compared with NiFe_2O_4 , the solubility of Al_2O_3 is much higher than that of Fe_2O_3 , but the Al_2O_3 has no effect on the purity of aluminium.

Received date: 2005-09-26

Biography: WANG Zhao-wen(born in 1964), Male, Professor, Doctor.

The experiments also examined the technical conditions, which can get better performance of the anode and tested the performance of the cermet to review the application prospect of the kinds of inert anodes based on NiAl_2O_4 and NiFe_2O_4 .

2 Fabrication of anodes

2.1 The hot pressing process

The NiO powder: high purity NiO 99%, $<10\ \mu\text{m}$; The Cu powder: high purity Cu $>99.8\%$, 200 mesh; The Ni powder: high purity Ni $>99.5\%$, 100–200 mesh; the Al_2O_3 powder: high purity $\text{Al}_2\text{O}_3 >99\%$; Fe_2O_3 powder: high purity $\text{Fe}_2\text{O}_3 >99\%$.

The NiAl_2O_4 and NiFe_2O_4 spinel were prefabricated in the laboratory. The mixture composed of NiO and Al_2O_3 or NiO and Fe_2O_3 powders was blended in a nylon vessel for 50 h using alcohol as the dispersant. An organic dispersant was used rather than water, because water may cause oxidation of the metal particles. And then the mixture was calcined at 1200°C in air for 2 h to form nickel aluminate or nickel ferrite. The metal powders (Cu+Ni) and the NiO additive were added to the calcined powder, and the mixture was again transferred to a ball mill and milled in a similar dispersant for an additional 50 h before drying and screening through a 320 mesh screen.

Hot pressing was used to prepare the cermet inert anodes based on the NiAl_2O_4 and NiFe_2O_4 spinel.

2.2 The characteristics of the anode samples

Tables 1 and 2 show the density of nickel aluminate-based and nickel ferrite-based cermet samples under different conditions, respectively.

Table 1 Density of the sintered nickel aluminate-based cermet samples under different conditions

No.	Sintering temperature/ $^\circ\text{C}$	Pressure/MPa	Practical density(PD) /($\text{g}\cdot\text{cm}^{-3}$)	Theoretical density(TD) /($\text{g}\cdot\text{cm}^{-3}$)	PD/TD/%
1	1300	25	4.825	4.86	99.3
2	1350	25	4.852	4.86	99.8
3	1400	25	4.692	4.86	96.5

Table 2 Density of the sintered nickel ferrite-based cermet samples under different conditions

No.	Sintering temperature/ $^\circ\text{C}$	Pressure/MPa	Practical density(PD) /($\text{g}\cdot\text{cm}^{-3}$)	Theoretical density(TD) /($\text{g}\cdot\text{cm}^{-3}$)	PD/TD/%
4	1000	18	6.1597	6.1597	92.24
5	1100	22	6.0550	6.1597	98.30
6	1100	18	6.1381	6.1597	99.65
7	1200	22	5.8080	6.1597	94.29

According to Table 1, the nickel aluminate-based cermet anode samples have low pore ratio, which is helpful to enhance the cermet performance. The density of the sample No. 2 is higher than No. 1 and close to the theoretical value. According to the plastic fluxion theory of compact processing^[14], increasing temperature will result in higher product density at the same operating pressure. The creep theory of compact processing says that increasing temperature will encourage grain growth, in contrast to the compact process which is controlled by diffusion^[14]. But when preparing sample No. 3, the temperature was higher and but a lower density was obtained. The reason for this anomaly is that the melting point of Cu is relatively low and the wetting characteristic of Cu toward ferrous nickel is poor, so that metallic Cu was lost from the

sample at high temperature.

According to Table 2, nickel ferrite-based cermet anode samples have higher pore ratio than the nickel aluminate-based ones. The theory that increasing temperature will result in higher product density at the same operating pressure was showed more obviously. Metal bleed-out at high temperature was also observed. Thus, controlling the temperature and choosing an appropriate pressure are the keys to obtaining good samples in hot pressing.

The electrical conductivity versus temperature was measured with a four-point technique^[5]. The Ar gas protected the samples from oxidation at high temperature. The temperature at which the measurements were carried out ranged from 400 °C to 1000 °C. To conduct the measurements at any given temperature, the sample was held for 5 min at the temperature of measurement, and the measurements were conducted starting with the lowest temperature. Figs. 1 and 2 show the electrical conductivity of nickel aluminate-based and nickel ferrite-based cermet samples versus temperature, respectively.

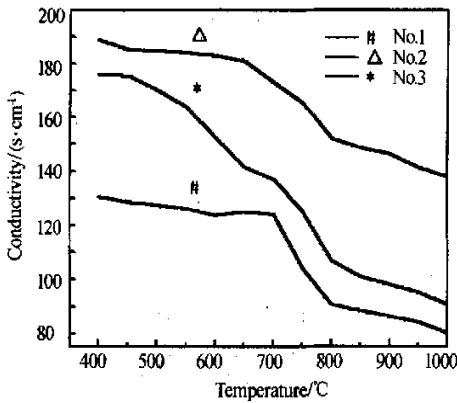


Fig. 1 Electrical conductivity versus temperature for the nickel aluminate-based samples

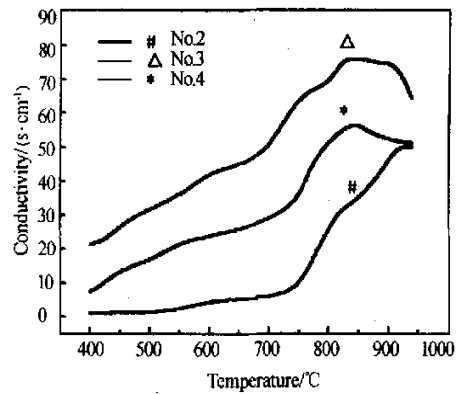


Fig. 2 Electrical conductivity versus temperature for the nickel ferrite-based samples

According to Fig. 1, in the low temperature range, below 600 °C, the conductivity of the nickel aluminate-based samples was significantly higher. The electrical conductivity of all samples was higher than $80 \text{ S} \cdot \text{cm}^{-1}$ at about 900 °C. The electrical conductivity of the best sample is higher than $140 \text{ S} \cdot \text{cm}^{-1}$ at about 900 °C. No remarkable change took place with rising temperature. From Fig. 1 a high sintering temperature is advantageous to get a better electrical conductivity. It can be concluded from Fig. 1 that the density of the sample has a great effect on the electrical conductivity, and the sample has the characteristics of metallic resistance. The electrical conductivity of the samples decreased with declining metal content in the anodic inner, so the metal is the main conductor of the cermet anode. To get a better electrical conductivity, the key is whether the metal network is continuous or not.

Fig. 2 shows that the electrical conductivity of the nickel ferrite-based samples increases with increasing temperature. At 900–1000 °C the electrical conductivities were all $40\text{--}80 \text{ S} \cdot \text{cm}^{-1}$. It can also be seen that the electrical conductivity changed remarkably at 720–750 °C. This highlights the varying conductivity of ferrous nickel spinel^[5]. From Fig. 2, it can be seen that Sample No. 6, the sample with the highest density has the best conductivity values. This highlights the need to achieve high density in cermet materials.

3 Electrolysis testing and discussions

3.1 Testing in electrolytic cells

The optimum technique was adopted to manufacture the two kinds of cermet anode.

The electrolytic cells for nickel aluminate-based and nickel ferrite-based cermet samples are shown schematically in Figs. 3 and 4, respectively. These designs ensure uniform distribution of the anode current density and sufficient cathode current density ($>0.33 \text{ A/cm}^2$)^[16]. Electrolysis was run in a tubular type of resistance furnace. The electrolysis temperature was $(900 \pm 5)^\circ\text{C}$, which was monitored during the experiment using a Pt/Pt-10%Rh thermocouple. The electrolyte was prepared from technical grade cryolite, added technical grade aluminium fluoride to achieve $\text{CR}=1.8$, technical grade CaF_2 , technical grade LiF and technical grade Al_2O_3 and the composition is: 3% CaF_2 , 5% LiF, 5% Al_2O_3 (mass fraction), with the balance being cryolite ($\text{CR}=1.8$).

During electrolysis, alumina was added every 30 min and the amount added was based on the electrolytic consumption rate at 60% cathodic current efficiency. Aluminium was not added to the crucible prior to commencement of experiments.

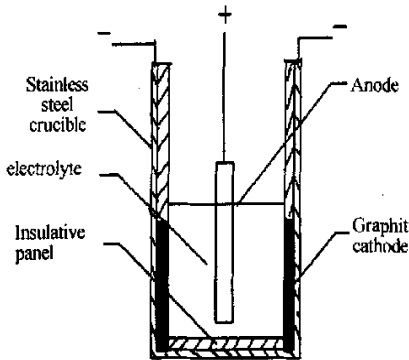


Fig. 3 Electrolysis cell for NiAl_2O_4 -based anode

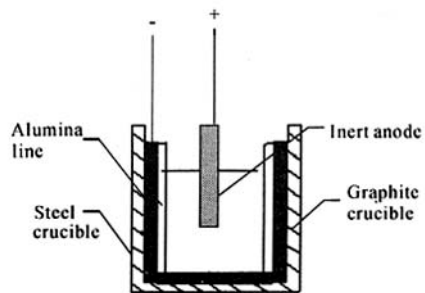


Fig. 4 Electrolysis cell for NiFe_2O_4 -based anode

3.2 Results and discussions

3.2.1 Nickel aluminate-based anode sample

The anode before and after electrolysis is shown in the Fig. 5. It can be seen that some parts swelled from the anode substrate and there are cracks in the anodic surface. Samples of the electrolyte were taken with a graphite rod every 1 h during the electrolysis. The graphite rod has no effect on the electrolyte composition. The main contaminants (Cu and Ni) were measured by chemical analysis (ICP). The results are shown in Fig. 6. A metal sample was also measured by the same means, and the result was: 0.251% Ni (mass fraction) and 0.483% Cu (mass fraction).

From Fig. 6, it can be seen that in the beginning the amounts of contamination (Ni and Cu) are higher than those in the following stage. But the amount did not reach saturation in the electrolyte. The amount of the metal elements (Ni and Cu) was low in the electrolyte from the anode due to the oxidation by the oxygen originating from the electrochemical reaction. In the process of electrolysis, the amounts also changed and reached the highest point at the 6th hour. From then on the amount of contamination was declining steadily. The reason can be concluded from the following: the metal amount in the anodic outer part is particularly high for hot pressing, the metals dissolved into the electrolyte as metal oxides. Then the contami-

nation in the electrolyte leveled off by the loss of the outer metals. Then the contamination decreased again for the reduction of the metal oxides on the cathode and reached a steady value in the following period. But in the following stage the cell voltage was steady, and the electrolysis was in a steady period. From Fig. 7 the cell voltage was lower in the beginning and then reached a steady value after passing the highest point. The reason can be concluded from the following; in the beginning the anodic resistance is low because of the high metal content in the outer section. Because the metal oxide reacted at the anodic surface, the cell voltage was increasing with the rising anodic resistance due to metal oxidation. When the metal oxide dissolved into the electrolyte, the matrix took part in the electrochemical reaction at the interface between the anode and the electrolyte. The conductivity of the matrix was better than that of the metal oxide, and then the cell voltage began to decrease and reached a steady value.

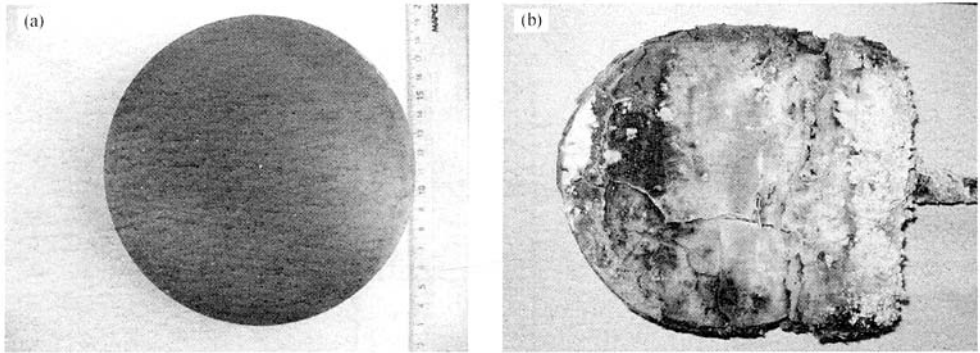


Fig. 5 Nickel aluminate-based anode sample before and after electrolysis
(a) — Before electrolysis; (b) — After electrolysis

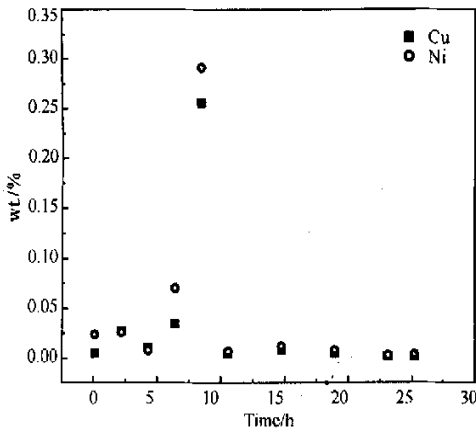


Fig. 6 The contaminations in the electrolyte versus the electrolysis time for Nickel aluminate-based anode sample

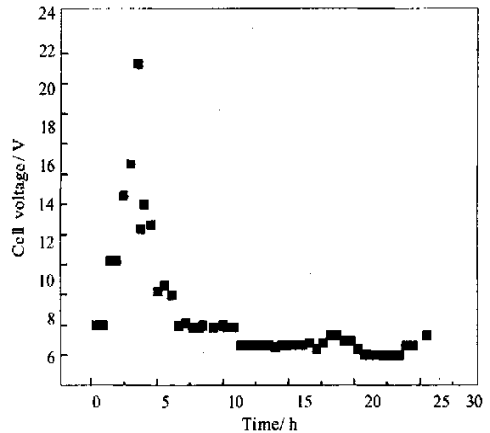


Fig. 7 The cell voltage versus the electrolysis time for nickel aluminate-based anode sample

Delamination took place in the outer part of the anode during electrolysis, which showed the corrosion behavior resulted from the electrolyte. The relation described above between the electrical conductivity and the density of the samples, the metals played an important role in the electrical conductivity. On the anodic

surface the active oxygen atom that was generated by oxidation of $\text{Al}_x\text{O}_y\text{F}_z^{(2y+x-3z)-}$ ions, oxidized the metal on the surface (Ni in particular). The new phase NiO generated in the anode, which can be indicated by the metallic peaks declining and the NiO peaks enhancing in Fig. 8. The new phase made the anodic surface loose. And in the electrolyte the contamination increased by the dissolution of loose part of the anode. The electrolytic reaction took place from the surface to the interior. And when it reached a certain depth, the corrosion got the balance for the metal loss. Delamination took place resulting from the difference thermal expansion coefficient of different phases between the outer anode and the inner anode. The anode based on the NiAl_2O_4 spinel can be run steadily and the contamination is low, so the anode delamination is the key to stand against the electrolyte. The performance of corrosion resistance can be enhanced and the anodic life can be prolonged. In order to get the target, a more uniform metal distribution is needed by improving the hot pressing technique (the pressure, the temperature and the holding time), to give increased corrosion resistance of the anode.

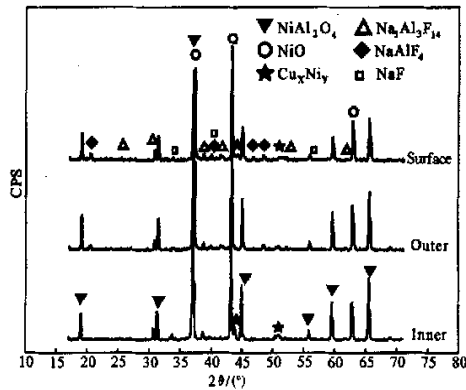


Fig. 8 XRD of the Nickel aluminate-based anode sample after electrolysis

3.2.2 Nickel ferrite-based anode sample

The anode before and after electrolysis is shown in the Fig. 9. Cracks was also found on the anode surface and some parts swelled from the anode substrate. XRD of nickel anode sample before and after electrolysis is showed in Fig. 10.

From Fig. 10, the intensity of diffraction peaks of Cu_xNi_y decreased sharply; the content of metals decreased gradually from inner to outer part and CuFe_2O_4 appeared on anode surface. AlF_3 was found on the surface of anode. NiF_2 that formed on the surface dissolved in the electrolyte, so there was no diffraction peak of NiF_2 on anode surface, and FeF_3 is gaseous so there was no diffraction peak of FeF_3 as well. $\text{Al}_x\text{O}_y\text{F}_z^{(2y+x-3z)-}$ ions in electrolyte moved to anode in the electric field, and then oxygen atoms disengaged from $\text{Al}_x\text{O}_y\text{F}_z^{(2y+x-3z)-}$ ions and became oxygen ions by losing their electrons. Meantime, $\text{AlF}_4^{(x-3)-}$ reacted with Fe^{3+} , Ni^{2+} in the anode. Structure of nickel ferrite was therefore destroyed. Fe^{3+} , Ni^{2+} reacted with F^- and then formed FeF_3 , NiF_2 . Therefore, it was $\text{Al}_x\text{O}_y\text{F}_z^{(2y+x-3z)-}$ ions in electrolyte that corroded the matrix of anode.

The effect of anodic current density was also studied, Table 3 gives the amount of contaminants in the aluminium produced. It can be seen that the degree of corrosion of the anode increased with increasing current intensity from 0.8 A/cm^2 to 1.2 A/cm^2 . In the melt the distribution of the amount of contaminant is close to that in the aluminium produced, with Fe being the main contaminant. The contaminant is derived from the metal oxides originating from the anode. The anode matrix consists of the ferrous nickel spinel

which has a low solubility in the cryolite-alumina melt. The contaminants went into the melt due to the dissolution reaction between the metal oxides and the melts given by Equation (1).

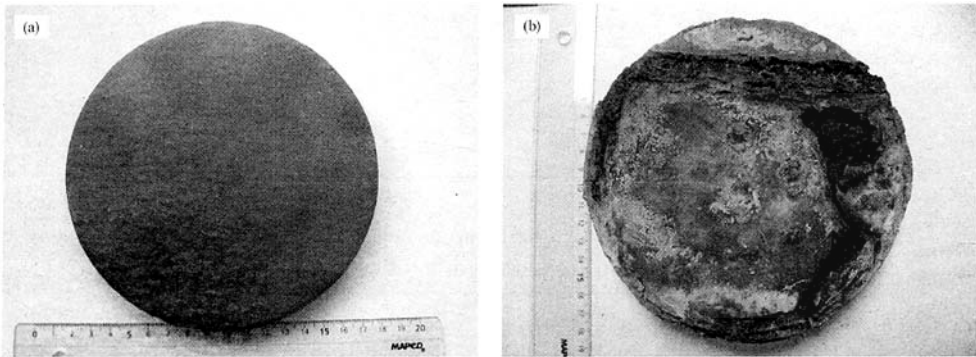


Fig. 9 Nickel ferrite-based anode sample before and after electrolysis
(a)—Before electrolysis; (b)—After electrolysis

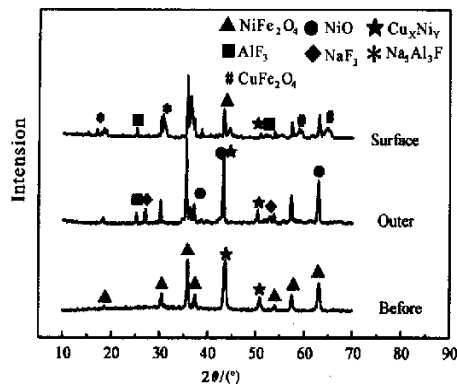


Fig. 10 XRD of nickel ferrite-based anode before and after electrolysis

According to the Tables 3 and 4, more Fe_2O_3 dissolves in the melt than the other contaminants. Among these metal oxides the solubility of Fe_2O_3 is much higher than those of NiO and CuO in the cryolite-aluminium melts. Fe_2O_3 exits as ferrous nickel in the anode. It is apparent that the structure of the ferrous nickel spinel is destroyed thus causing more Fe_2O_3 to dissolve in the melt. The anode electrical conductivity is enhanced due to the addition of the metals. The metals are the main conductors, as the electrical conductivity of ferrous nickel spinel is about $0.5 \text{ S} \cdot \text{cm}^{-1}$ at 900°C ^[15]. The mechanism of electrical conduction in the ferrous nickel spinel is due to the electron transport between Fe^{3+} ions locating in the octahedral interstices^[15]. At higher current intensity, the activity of Fe^{3+} ions is enhanced. Under the condition of high current intensity the Fe^{3+} ions are better able to react with the melt, resulting in the destruction of spinel structure and a resulting increase of the Fe contamination in the aluminium produced. The amount of Cu contamination also increased with an increase in the anode current density. During the electrolysis the metal Cu can transfer from the inside of the anode to the outside of the anode due to the high Cu mobility^[9]. Thus, there is a Cu-rich zone on the anode surface. With increasing current intensity, Cu on the anode surface becomes richer. Thus, more Cu dissolves in the melt, resulting in an increase in the level of Cu con-

tamination in the aluminium produced.

Table 3 Amount of contaminants in the aluminium under different anode current density for nickel ferrite-based anode

No.	Current density /(A · cm ⁻²).	Impurity content (mass fraction)/ %		
		Fe	Ni	Cu
a	0.8	0.105	0.097	0.055
b	1.0	1.530	0.130	2.490
c	1.2	1.720	1.310	3.570

Table 4 Amount of contaminants in the melt under anode current density 0.8 A/cm² for nickel ferrite-based anode

Contaminations	Fe	Ni	Cu
Amount (mass fraction) / %	0.070	0.013	0.039

4 Conclusions

(1) By hot pressing cermet anodes based on the NiAl₂O₄ or NiFe₂O₄ spinel above 99% relative density can be obtained;

(2) The electrical conductivity of NiAl₂O₄-based anode is above 140 S · cm⁻¹ and that of FeAl₂O₄-based anode is about 75 S · cm⁻¹ at 900 °C;

(3) The nickel aluminate-based cermet anode can be run steadily. The new phase NiO causes swelling and delamination of the outer part of the anode.

(4) The degree of corrosion increase with an increase in the anode current density from 0.8 A/cm² to 1.2 A/cm² for the nickel ferrite-based cermet anode. The activity of Fe³⁺ ions increased due to an increase in the anode current density, resulting in the corrosion of the ferrous nickel spinel and the level of contamination in the aluminium produced. With an increase in the anode current density, Cu can be enriched in the outer surface of the anode due to high Cu mobility. The results in an increase in the level of copper contamination in the aluminium produced.

References

- [1] Pawlek R P. Inert anode; an update. TMS, Light Metals, 2002, 449-456.
- [2] Tabercaux A T. Anode effect, PFCs, global warming and the aluminium electrolysis[J]. JOM, 1994, 46(11): 30-31, 33-34.
- [3] Zhao Q, Qiu Z X, Wang Z W. Materials design of inert anode in aluminium electrolysis[J]. Light Metals, 2002, (11): 42-44.
- [4] Kvande H. Inert anodes in aluminium electrolysis cells[J]. TMS, Light Metals, 1999, 369-376.
- [5] Olsen E, Thonstad J. Nickel ferrite as inert anodes in aluminium electrolysis; Part_ Materials fabrication and preliminary testing[J]. Journal of Applied Electrochemistry, 1999, 29(3): 293-299.
- [6] Hryn J N, Pellin M J. A dynamic inert metal anode[J]. TMS, Light Metals, 1999, 377-381.
- [7] Keniry J. The economics of inert anodes and wettable cathodes for aluminum reduction cells[J]. JOM, 2001, 53(4): 43-47.
- [8] Kvande H, Haupin W. Inert anodes for Al smelters: energy balances and environmental impact[J]. JOM, 2001,

53(4): 29–33.

- [9] Lorentsen Odd-Arne, Thonstad J. Electrolysis and posttesting of inert cermet anodes[J]. TMS, Light Metals, 2002, 457–462.
- [10] Sekhar J A, *et al.* Micropyretically synthesized porous nonconsumable anodes in the Ni-Al-Cu-Fe-X system[J]. TMS, Light Metals, 1996, 347–354.
- [11] Thonstad J, Olsen E. Cell operation and metal purity challenges for the use of inert anodes[J]. JOM, 2001, 53 (4): 36–38.
- [12] Sadoway D R. Inert anodes for the Hall-Heroult cell; the ultimate materials challenge[J]. JOM, 2001, 53 (4): 34–35.
- [13] Shi Z N, *et al.* Copper-nickel superalloys as inert alloy anodes for aluminum electrolysis[J], JOM, 2003, 54 (11): 66–69.
- [14] Huang P Y. Powder metallurgy mechanism[M]. Beijing: Metallurgy Industry Press, 1997.
- [15] Han Y S. Preparation and investigations of inert anode applied in aluminium production and porous ceramics[D]. Beijing: Tsinghua University, 2003.
- [16] Qiu Z X. Theory and application of aluminium electrolysis[M]. Xuzhou: China Mining and Technology Press, 1998.